Cambridge Centre for Computational Chemical Engineering

University of Cambridge

Department of Chemical Engineering and Biotechnology

First-principles thermochemistry for the combustion of TiCl$_4$ in a methane flame

Tim S. Totton [1]   Raphael Shirley [1]   Markus Kraft [1]

released: July 28, 2010

[1] Department of Chemical Engineering and
Biotechnology
University of Cambridge
New Museums Site
Pembroke Street
Cambridge, CB2 3RA
UK
E-mail: mk306@cam.ac.uk

c4e

Abstract

This work presents thermochemical data for many of the intermediates in the early stages of the combustion of titanium tetrachloride ($TiCl_4$) in the presence of residual species from a methane flame. An algorithm developed for previous work is employed to ensure that all possible species are considered, reducing the probability of neglecting important species. Thermochemical data and enthalpies of formation are calculated for 141 new species using density functional theory (DFT) and statistical mechanics. Equilibrium calculations are performed to try to identify which intermediates are likely to be most prevalent in the high temperature industrial process. The ten species with the highest equilibrium compositions are identified and presented in the paper. These species, $TiCl_3OH$, $Ti_2O_2Cl_3OH$, $Ti_2OCl_4(OH)_2$, $TiCl_2OH$, $TiOClOH$, $TiCl_2(OH)_2$, $TiOCl_2OH$, Ti_2O_3ClOH, $Ti_2O_2Cl_2(OH)_2$, and $TiCl(OH)_2$, along with the original $Ti_xO_yCl_z$ species are likely to be the most important species involved in the kinetic model. Data for the remaining species is provided as Supplemental Material. The abundance of $Ti_iO_jCl_kH_l$ species is high considering the low amount of hydrogen present in the simulation and they are likely to have a significant impact on the process, something that has not been recognized in previous publications.

1

Contents

1 Introduction

Titanium dioxide (TiO_2) is widely used as a pigment, as a catalyst support, and as a photocatalyst. The combustion of titanium tetrachloride ($TiCl_4$) to synthesize TiO_2 nanoparticles is a multi-million tonne per year industrial process [6]. In this 'chloride' process, purified titanium tetrachloride is oxidized at high temperatures (1500–2000 K) in a pure oxygen plasma or flame to produce TiO_2 particles [5, 8, 19]. The overall stoichiometry of this oxidation process is

$$TiCl_4 + O_2 \longrightarrow TiO_{2\,(nanoparticles)} + Cl_{2\,(g)}. \tag{1}$$
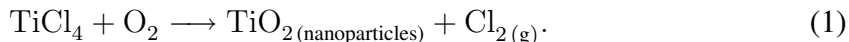
Although the chloride process is a mature technology, which has been used in industry since 1958, understanding of the gas-phase reactions of $TiCl_4$ in a flame remains incomplete [16]. Recently, West *et al.* have developed a detailed kinetic model for the chloride process using an oxygen plasma, including thermochemical data for the titanium oxychloride species involved [25, 30–32]. When a pure oxygen plasma is used these species will be sufficient for a kinetic model. However, when a flame is used to superheat the oxygen, the residual combustion species (in particular water) are likely to interact chemically with the titanium oxychloride species. It would be instructive to determine to what extent H and OH groups influence the intermediate species formed.

Recently there have been a number of experimental studies of TiO_2 particle formation via combustion in hydrocarbon flames. These include studies using $TiCl_4$ in methane [17] and propane flames [33], as well as the related titanium compound titanium tetraisopropoxide (TTIP) in methane flames [1, 15]. This work investigates $TiCl_4$ combustion in a methane flame. This decision was made because of the industrial use of $TiCl_4$ and the well understood nature of a methane flame which includes a detailed kinetic model [26]. Although this work concentrates on $TiCl_4$ in a methane flame the species investigated will be equally useful for the study of $TiCl_4$ and TTIP combustion in other flame environments.

The aim of this study is to provide gas-phase thermochemical data for important titanium species containing oxygen, chlorine and hydrogen ($Ti_iO_jCl_kH_l$). This data has been calculated from first principles using density functional theory (DFT) and statistical mechanics for an exhaustive list of 141 species. In order to ascertain the importance of particular species, equilibrium calculations have been used to identify the most abundant species in a methane flame environment.

2 Computational Method

2.1 Species Generation

No reaction scheme is available for the combustion of $TiCl_4$ in a hydrocarbon flame. It is therefore necessary to determine those species that could possibly be formed in such a system. This section describes the method we have used to generate an exhaustive list of all likely reacting species. We have recently developed a script to automatically generate species from a selection of existing species [23, 25].

Specifically, the method used here involved replacing chlorine atoms on a set of titanium oxychloride ($Ti_xO_yCl_z$) species with either hydrogen atoms or hydroxide groups. When generating the species, the only operation the algorithm performs at any given stage is the replacement of a single-bonded chlorine atom with a single-bonded hydrogen atom or a single bonded hydroxide group. We therefore used the same spin multiplicity as calculated for the original species of West *et al.* [30, 32].

Every possible combination of chlorine replacements in the original $Ti_xO_yCl_z$ species is considered. Figure 1 shows the result of applying this algorithm to the starting species $TiCl_4$. In order to remove any duplicates, an International Chemical Identifier (InChI) name, which can uniquely identify molecules of the same connectivity, is assigned to each species using OpenBabel [11, 22]. Duplicate species can then be automatically removed from the set by simply comparing the InChI names.

Each step of this process is fully automated using a combination of Python and Perl scripts. All the new species generated were checked manually to ensure no important species were absent. Conversely, this check also ensured that physically unrealistic species were identified and removed.
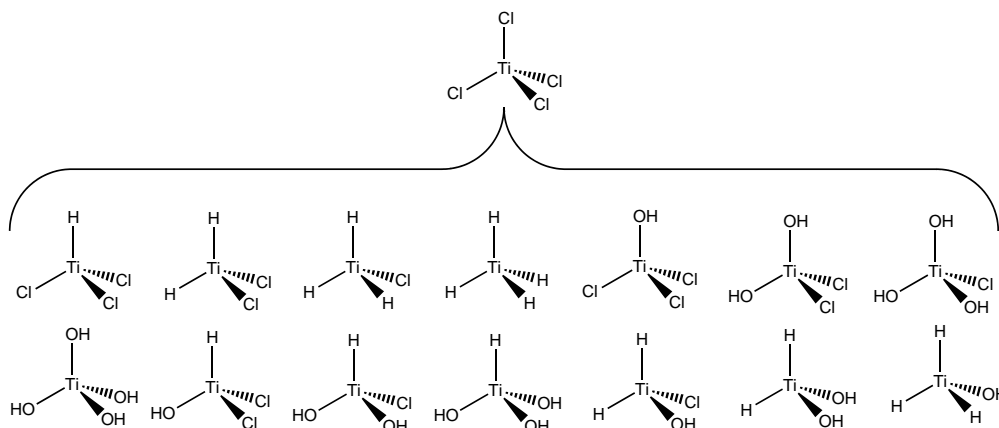

Figure 1: *Generating possible hydrogen-containing species from $TiCl_4$. Thermochemical data for all of these species is provided as Supplemental Material.*

4

2.2 Quantum Chemistry Calculations

Geometry optimization and molecular properties for all new species were calculated using density functional theory (DFT). Previous studies on the $Ti_xO_yCl_z$ system [25, 30, 32] indicate that the B97-1 [12] functional is the most reliable and accurate. Consequently, we have used this functional throughout the present study.

The basis set used for all DFT calculations was 6-311+G(d,p). This consists of the 6-311G basis set [18] for oxygen; the McLean-Chandler (12s,9p) (621111,52111) "negative ion" basis set [21] for chlorine; the Wachters-Hay all-electron basis set [13, 27] for titanium, using the scaling factors of Raghavachari and Trucks [24] and supplementary polarization functions and diffuse functions. Such a supplemented, triple-ζ basis set should be large enough to ensure that the basis set truncation error is comparable with, or smaller than, the inherent errors in the DFT [2].

All DFT calculations were carried out using the GAUSSIAN03 package [7]. The convergence threshold for the self consistent field was set to 10^{-8} Hartrees. The geometry optimization was considered to have converged if the root-mean-squared force on every atom was under 10^{-5} Hartrees/Bohr.

2.3 Statistical Mechanics and Equilibrium Composition

Heat capacities (C_p°), thermal enthalpy ($H(T) - H(0\ \text{K})$), and entropies (S°) were calculated for temperatures in the range 20-4000 K using the rigid rotator harmonic oscillator (RRHO) approximation, taking unscaled vibrational frequencies and rotational constants from the B97-1/6-311+G(d,p) calculations. The contribution of the excited electronic states to the partition function is ignored as in previous studies [25, 30, 32], where titanium containing-species have been shown to not possess low energy excited states.

Polynomials in the NASA [10] form were fitted to C_p° (T)/R, H° and S° over the temperature ranges 20-T_x K and T_x-4000 K, constrained to ensure that all three functions are continuous and smooth across the boundary temperature, T_x, which was varied to optimize the fit. Using these NASA polynomials, the equilibrium composition as a function of temperature was calculated using the open source software Cantera [9].

3 Results and Discussion

3.1 Geometries

Converged geometries and molecular properties were found for 141 new species. All this information in the form of GAUSSIAN03 output files and MDL Molfiles are provided in the Supplemental Material where species are identified by the unique SMILES name [28, 29] generated using OpenBabel [11]. For a small number of DFT calculations the self-consistent field (SCF) did not converge within 400 iterations. Such species were investigated manually and in all such cases were deemed to be physically unreasonable. Typically they involved two atoms within half an Ångstrom of each other or involved one species which had split into two molecules but retained the now unphysical multiplicity. These species accounted for approximately 10% of the total. A challenge for future studies will be to develop a system for automatically rejecting such species. For very large chemical systems it may be sensible to use a cheaper computational method in the first instance to perform this check.

In cases where multiple isomers exist for a given empirical formula, all isomers are included. This is because before running equilibrium composition calculations there is no straightforward way to determine which species are more important. Additionally, since they will take part in different reaction paths a future kinetic model may need to consider each isomer individually.

3.2 Enthalpy of Formation

The standard enthalpy of formation at 0 K, $\Delta_{\mathrm{f}} H_{0\,\mathrm{K}}^{\circ}$, can be determined by subtracting the energy of the species from the energy of its elements in their standard states as calculated using DFT. However this can lead to systematic errors in the DFT calculations propagating through to the final enthalpies. An alternative method is to use isodesmic reactions [23, 30] which relate the species with unknown enthalpy to other species with known enthalpy. In an isodesmic reaction the type and number of bonds broken are the same as those of bonds formed. As the products and reactants have similar electronic structures, systematic errors associated with given bonds are largely canceled out [14].

In this work, we have tried to relate all of the new species using isodesmic reactions with species with known enthalpy from the literature. It has not always been possible to find purely isodesmic reactions as there is not a sufficiently large pool of species with known enthalpy to allow such reactions to be found. In particular, we have not been able to find species with known enthalpy containing the $\mathrm{Ti-H}$ bond, which means isodesmic reactions cannot be found for species containing this bond. The pool of species with known enthalpy is given in Table 1. In the case where an isodesmic reaction is not available, an alternative reaction has been found which minimizes the total number of different bonds between products and reactants. Multiple reactions have been found with the lowest number of bond changes and the final enthalpies represent the enthalpy of formation averaged over all the possible reactions. A full list of enthalpies of formation for the 141 new species is given in the Supplemental Material, and a subset corresponding to the ten most

abundant species in the equilibrium calculations (Section 3.4) is given in Table 2.

The standard deviations associated with the standard enthalpies of formation for the new species vary widely from 5 kJ/mol to 122 kJ/mol. For the majority of species with a large standard deviation it is mainly due to one reaction giving a markedly different enthalpy to all the others. This is due to one or more of the known species having a spurious enthalpy. This is not unexpected as inconsistences in experimentally obtained enthalpies of formation have previously been observed [30].

At high temperature, where entropy is the dominant contribution to the Gibbs energy, the equilibrium compositions are relatively insensitive to the enthalpy of formation. While standard deviations of up to 100 kJ/mol in the enthalpy are significant, the large errors tended to be associated with unstable species (Section 3.4). These values correspond to a standard deviation in the mean of up to 40 kJ/mol. Errors of this scale are expected and are broadly consistent with those obtained by Phadungsukanan *et al.* [23] for silica species. A basic sensitivity analysis was conducted whereby enthalpies of these species were varied by this amount and, while the equilibrium concentrations were affected, the conclusions remained unchanged.

Table 1: *Literature values for standard enthalpies of formation at* 298.15 *K used to find reactions with low numbers of bond changes to calculate standard enthalpies of formation for new species. Errors are included where available.*

Species	$\Delta_f H^\circ_{298.15\,K}$ kJ/mol	Error kJ/mol	Reference
TiOCl	−274		[30]
$TiOCl_2$	−598		[30]
$TiOC_3$	−639		[30]
TiO_2Cl_2	−558		[30]
TiO_2Cl_3	−774		[30]
$Ti_2O_2Cl_3$	−1257		[30]
$Ti_2O_2Cl_4$	−1552		[30]
$Ti_2O_3Cl_2$	−1331		[30]
$Ti_2O_3Cl_3$	−1418		[30]
$Ti_2O_2Cl_5$	−1272		[32]
$Ti_2O_2Cl_6$	−1503		[32]
$TiCl_4$	−763.16		[3]
$TiCl_3$	−539.32		[3]
$TiCl_2$	−237.23		[3]
TiO_2	−305.43		[3]
ClOCl	87.86		[3]
OClO	104.60		[3]
ClOH	−74.48		[3]
H_2O	−241.826	±0.040	[4]
HCl	−92.31	±0.10	[4]
OH	38.99		[3]
Cl	121.301	±0.008	[4]
O	249.18	±0.10	[4]

3.3 Thermochemistry

A full list of computed molecular and standard thermochemical data for species convergent under geometry optimization using the B97-1 functional with the 6-311+G(d,p) basis

Table 2: *Standard enthalpies of formation at 0 K and 298.15 K, with standard deviation and number of reactions used with the corresponding number of bond changes for the 10 highest-concentration species calculated at the B97-1/6-311+G(d,p) level of theory for stable electronic ground states. To find corresponding information in the Supplemental Material use the SMILES names provided in Figure 3.*

Species	$\Delta_\mathrm{f} H^\circ_{0\,\mathrm{K}}$ kJ/mol	$\Delta_\mathrm{f} H^\circ_{298.15\,\mathrm{K}}$ kJ/mol	Standard Deviation kJ/mol	No. of reactions	No. of bond changes
$TiCl_3OH$	−941	−917	14	6	0
$Ti_2O_2Cl_3OH$	−1741	−1708	14	4	0
$Ti_2OCl_4(OH)_2$	−1936	−1893	56	6	0
$TiCl_2OH$	−719	−699	24	6	0
$TiOClOH$	−742	−724	34	7	0
$TiCl_2(OH)_2$	−1079	−1054	28	6	0
$TiOCl_2OH$	−793	−770	28	6	0
Ti_2O_3ClOH	−1545	−1518	64	6	0
$Ti_2O_2Cl_2(OH)_2$	−1866	−1831	43	6	0
$TiCl(OH)_2$	−850	−829	29	6	0

set are presented in the Supplemental Material. Table 3 shows this data for the ten most abundant species in the equilibrium composition (Section 3.4).

3.4 Equilibrium Composition

Equilibrium compositions were calculated using NASA polynomials for: 141 new species as calculated in this work, those from the titanium oxychloride reaction mechanism presented by West *et al.* [32], and all of the species except those containing nitrogen from the GRI-Mech methane mechanism [26]. The West *et al.* reaction mechanism includes NASA polynomials for $TiCl_x$ ($x = 1, \ldots, 4$), TiO, TiO_2, chlorine oxides and standard gases, taken from the NASA database [20]. Additionally the polynomials for HCl from the NASA database were used. The GRI-Mech species were used because they include all important residual combustion species. For species which exist in both the GRI-Mech mechanism and the West *et al.* mechanism, the data used is taken from West *et al.*.

Computed equilibrium data calculated over the temperature range of 500–3500 K are shown in Figure 2 for a fuel lean mixture initially containing 48.5 mol % $TiCl_4$, 3 mol % CH_4, and 48.5 mol % O_2 at 101.3 kPa. These conditions are typical in industry where a lean hydrocarbon flame is used to superheat the oxygen and the reaction with $TiCl_4$ is close to stoichiometric. Figure 2(a) shows only the upper part of the concentration plot in order to show the specific species that are most stable. This plot clearly shows that species containing both titanium and hydrogen are of considerable importance. This is true for all of the flame environments investigated. For clarity, the individual species concentrations have been collected in Figure 2(b). The following groups were used: GRI-Mech species (excluding O, O_2, O_3, taken from West *et al.*), West *et al.* species split into TiO_xCl_y monomers, $Ti_2O_xCl_y$ dimers, O_xCl_y species/HCl, and the new species presented in this work separated into $TiO_xH_yCl_z$ monomers and $Ti_2O_xH_yCl_z$ dimers. The precise species used in each group are tabulated in the Supplemental Material which includes references

Table 3: *Standard entropy at 298.15 K, $S^{\circ}_{298.15\ K}$, and molecular properties for the 10 highest-concentration species calculated at the B97-1/6-311+G(d,p) level of theory for stable electronic ground states. The electronic degeneracy, g, and the rotational symmetry, s, are included. To find corresponding information in the Supplemental Material use the SMILES names provided in Figure 3.*

| species	$S^{\circ}_{298.15\ K}$ J/mol K	g	s	rot. const. GHz	vibrational frequencies cm^{-1}
$TiCl_3OH$	386.0	1	1	1.5727 1.5474 1.1256	101.06, 113.62, 115.97, 136.66, 157.85, 200.48, 224.21, 402.83, 483.16, 492.26, 828.6, 3944.84
$Ti_2O_2Cl_3OH$	460.4	1	1	1.1879 0.5062 0.3801	43.34, 72.96, 97.9, 109.55, 109.62, 157.42, 165.47, 219.24, 245.55, 278.26, 321.47, 330.37, 432.67, 441.93, 508.43, 545.41, 716.4, 735.29, 779.19, 809.18, 3941.09
$Ti_2OCl_4(OH)_2$	575.2	1	1	0.7414 0.2997 0.2867	5.01, 18.38, 21.39, 84.21, 106.09, 109.98, 116.43, 126.67, 137.77, 151.28, 161.67, 190.33, 232.29, 249.37, 274.81, 284.7, 342.19, 407.01, 439.06, 485.41, 488.62, 498.47, 773.14, 812.75, 899.08, 3924.35, 3948.95
$TiCl_2OH$	351.3	2	2	3.9435 1.9430 1.3017	89.61, 101.74, 134.39, 166.55, 367.6, 383.37, 478.74, 794.8, 3973.44
$TiOClOH$	331.6	1	1	7.5435 2.6268 1.9484	34.4, 145.65, 224.39, 420.53, 519.71, 548.94, 751.0, 1079.95, 3919.73
$TiCl_2(OH)_2$	383.5	1	1	2.4046 1.6691 1.3998	108.56, 120.51, 153.55, 156.39, 183.08, 188.95, 263.3, 293.99, 375.98, 434.04, 480.5, 777.73, 812.37, 3925.11, 3943.23
$TiOCl_2OH$	394.7	2	1	2.4723 1.7180 1.3842	21.26, 120.99, 126.31, 131.29, 166.06, 181.5, 345.92, 424.07, 479.52, 678.21, 804.42, 3945.81
Ti_2O_3ClOH	409.3	1	1	2.2879 0.8596 0.7099	67.67, 117.03, 140.1, 151.2, 162.95, 163.59, 225.91, 266.65, 313.61, 386.18, 468.56, 496.52, 699.72, 729.63, 755.33, 777.45, 1060.05, 3986.56
$Ti_2O_2Cl_2(OH)_2$	467.8	1	1	1.4469 0.5871 0.4531	49.32, 83.22, 112.76, 116.13, 119.33, 140.78, 164.85, 193.31, 223.08, 240.26, 260.1, 261.49, 323.14, 366.32, 440.59, 447.6, 545.44, 707.53, 739.88, 764.57, 772.79, 812.27, 3963.01, 3966.45
$TiCl(OH)_2$	360.3	2	1	5.6454 2.7264 1.8385	88.14, 100.44, 134.4, 160.77, 272.28, 352.64, 386.3, 413.72, 737.37, 784.81, 3989.12, 3993.19

to the original sources. There are 201 species overall in the system, some 141 of which are those presented in this work.

Geometries of the ten most abundant species containing hydrogen (in terms of mole fraction) over the temperature range 1500–2500 K are shown in Figure 3. Both empirical formula and SMILES format names are given to help the reader associate empirical names used in the paper with the SMILES used in the Supplemental Material. A number of these hydrogen containing species are present at comparable or greater levels than the titanium oxychloride species. In an industrial context, where the gases are essentially at equilibrium because particle formation is rate-limiting, some of these species are likely to play an important role in the gas kinetics and nucleation process.

A number of different initial compositions were experimented with, including methane lean flames with very low $TiCl_4$ concentrations, as typically used in experiments, methane rich flames with larger $TiCl_4$ concentrations, as well as methane lean flames with larger $TiCl_4$ concentrations ($Ti:O_2 = 1:1$) which have industrial relevance. As expected the relative abundance of hydrogen in the initial composition has a large impact on the species present at equilibrium. The more hydrogen present, the higher the concentrations of the
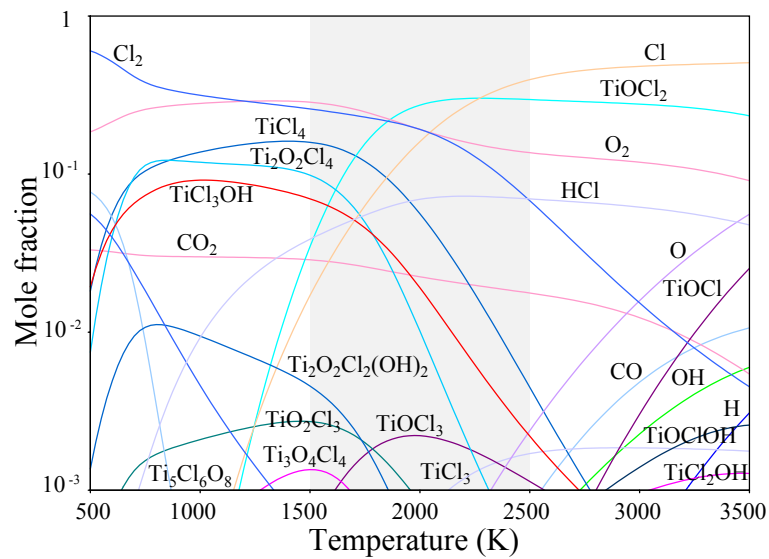
(a) Detailed equilibrium concentrations
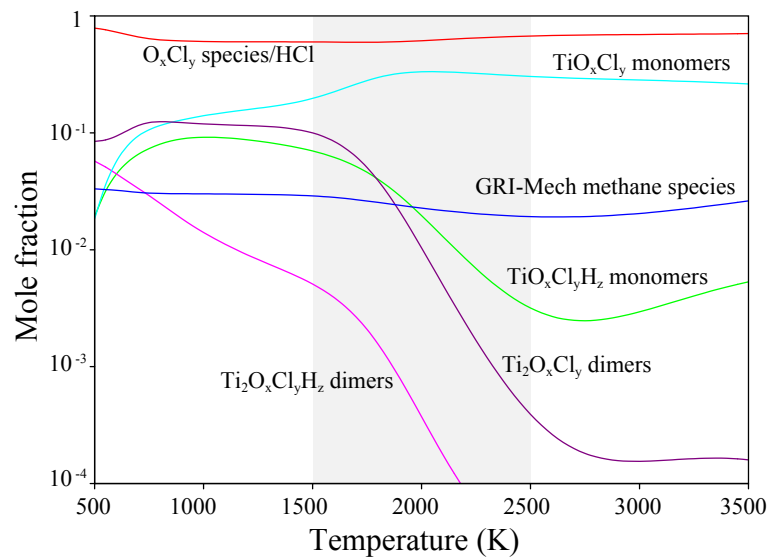
(b) Collated equilibrium concentrations

Figure 2: *Computed equilibrium for combustion of $TiCl_4$ in a methane flame. Initial concentrations are 48.5 mol % $TiCl_4$, 3 mol % CH_4, and 48.5 mol % O_2 at 101.3 kPa. Thermochemical data for $Ti_xO_yCl_z$ species from West et al. [32] and the NASA database [20]. All species from the GRI-Mech methane mechanism included [26]. The central grey band indicates the temperature range most relevant to industrial reactors.*
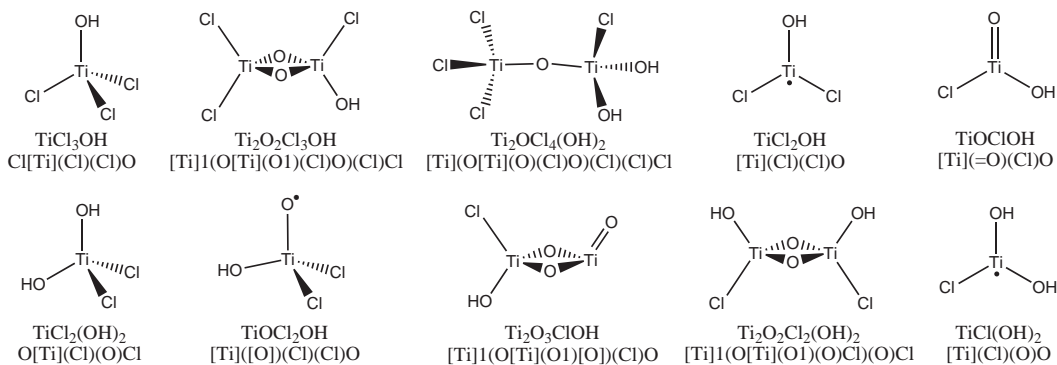
Figure 3: *Geometries of the ten most abundant new species over the temperature range 1500-2500 K. The Supplemental Material is all organized in terms of the SMILES system for naming molecules. These are reported here so that the reader can associate the more readable names used in the paper with the SMILES used in the Supplemental Material.*

new $Ti_iO_jCl_kH_l$ species compared to the existing $Ti_iO_jCl_k$ species. Conversely, the higher the initial concentration of oxygen, the lower the concentration of the new species and additionally within the new species hydroxide groups are preferred to the hydrides. Specifically, at a typical industrial reactor temperature of 2000 K the new monomers and dimers become more abundant than their titanium oxychloride counterparts when the initial CH_4 concentration rises above 3.8 % compared to stoichiometric $TiCl_4$:O_2 conditions. For this reason we recommend that the original kinetic model presented by West *et al.* is only applicable when hydrogen-containing species are at very low concentrations.

For the initial conditions presented in Figure 2, where the amount of hydrogen in the system is very low, the high concentrations of some hydrogen-containing species indicate the comparable thermodynamic stability of $Ti-OH$ bonds with $Ti-Cl$ bonds. $TiCl_3OH$ is the most abundant new species and is comparable to $TiCl_4$ and HCl and will be important to the system reaction kinetics. Of the ten most abundant new species, four are titanium dimers and therefore the presence of hydrogen is highly likely to play an important role in dimerization and subsequent particle growth.

4 Conclusions

This work has extended the detailed thermochemistry of the gas-phase titanium oxychloride species investigated by West *et al.* [30] to a similar system of hydrogen-containing species. These were not previously included in their work but play an important role in the industrial flame synthesis of TiO_2 where small amounts of residual combustion species are present. New molecular geometries have been proposed through automated species generation and investigated using density functional theory with the B97-1 functional and the 6-311+G(d,p) basis set. This enabled detailed thermochemical data to be computed for the generated species, which have not been reported in the literature and are difficult to obtain experimentally.

Using the thermochemical data, temperature-dependent equilibrium compositions were obtained through simulations at industrial operating conditions. A number of conclusions are made from these studies:

- Hydrogen containing species are stable and will exist at industrial and experimental conditions.

- $TiCl_3OH$, $Ti_2O_2Cl_3OH$, $Ti_2OCl_4(OH)_2$, $TiCl_2OH$, $TiOClOH$, $TiCl_2(OH)_2$, $TiOCl_2OH$, Ti_2O_3ClOH, $Ti_2O_2Cl_2(OH)_2$, and $TiCl(OH)_2$ are highlighted as ten of the most stable $Ti_iO_jCl_kH_l$ species for industrial conditions.

- Specifically $TiCl_3OH$ is the most abundant new species. It is hence likely to play an important role in the combustion synthesis of TiO_2 nanoparticles even when there is a relatively small amount of hydrogen, as in industrial flame reactors.

5 Acknowledgments

References

[1] O. Arabi-Katbi, S. Pratsinis, P. Morrison, and C. Megaridis. Monitoring the flame synthesis of TiO2 particles by in-situ FTIR spectroscopy and thermophoretic sampling. *Combustion and Flame*, 124(4):560–572, 2001.

[2] A. D. Boese, J. M. L. Martin, and N. C. Handy. The role of the basis set: Assessing density functional theory. *J. Chem. Phys.*, 119(6):3005–3014, Aug 2003. ISSN 0021-9606. doi:10.1063/1.1589004.

[3] M. W. Chase Jr. NIST-JANAF thermochemical tables, fourth edition. *J. Phys. Chem. Ref. Data*, Monograph 9:I–II, 1998.

[4] J. Cox, D. Wagman, and V. Medvedev. CODATA Key Values for Thermodynamics. Hemisphere Publishing Corp., New York, 1984.

[5] J. C. Deberry, M. Robinson, M. Pomponi, A. J. Beach, Y. Xiong, and K. Akhtar. Controlled vapor phase oxidation of titanium tetrachloride to manufacture titanium dioxide. US Patent 6,387,347, 2002.

[6] J. Emsley. *Molecules at an Exhibition*. Oxford University Press, 1999.

[7] M. J. Frisch, G. W. Trucks, H. B. Schlegel, G. E. Scuseria, M. A. Robb, J. R. Cheeseman, J. A. Montgomery, Jr., T. Vreven, K. N. Kudin, J. C. Burant, J. M. Millam, S. S. Iyengar, J. Tomasi, V. Barone, B. Mennucci, M. Cossi, G. Scalmani, N. Rega, G. A. Petersson, H. Nakatsuji, M. Hada, M. Ehara, K. Toyota, R. Fukuda, J. Hasegawa, M. Ishida, T. Nakajima, Y. Honda, O. Kitao, H. Nakai, M. Klene, X. Li, J. E. Knox, H. P. Hratchian, J. B. Cross, V. Bakken, C. Adamo, J. Jaramillo, R. Gomperts, R. E. Stratmann, O. Yazyev, A. J. Austin, R. Cammi, C. Pomelli, J. W. Ochterski, P. Y. Ayala, K. Morokuma, G. A. Voth, P. Salvador, J. J. Dannenberg, V. G. Zakrzewski, S. Dapprich, A. D. Daniels, M. C. Strain, O. Farkas, D. K. Malick, A. D. Rabuck, K. Raghavachari, J. B. Foresman, J. V. Ortiz, Q. Cui, A. G. Baboul, S. Clifford, J. Cioslowski, B. B. Stefanov, G. Liu, A. Liashenko, P. Piskorz, I. Komaromi, R. L. Martin, D. J. Fox, T. Keith, M. A. Al-Laham, C. Y. Peng, A. Nanayakkara, M. Challacombe, P. M. W. Gill, B. Johnson, W. Chen, M. W. Wong, C. Gonzalez, and J. A. Pople. Gaussian 03, Revision C.02, 2003. Gaussian, Inc., Wallingford, CT, 2004.

[8] R. A. Gonzalez, C. D. Musick, and J. N. Tilton. Process for controlling agglomeration in the manufacture of TiO_2. US Patent 5,508,015, April 1996.

[9] D. G. Goodwin. An open source, extensible software suite for CVD process simulation. In M. Allendorff, F. Maury, and F. Teyssandier, editors, *Chemical Vapor Deposition XVI and EUROCVD 14*, volume 2003-08 of *ECS Proceedings*, pages 155–162, Pennington, New Jersey, USA, 2003. The Electrochemical Society, The Electrochemical Society. URL code.google.com/p/cantera/.

[10] S. Gordon and B. J. McBride. Computer program for calculation of complex chemical equilibrium composition, rocket performance, incident and reflected shocks and

chapman-jouguet detonations. Technical Report NASA-SP-273, NASA, Glenn Research Center, Cleveland, OH, 1976. URL http://hdl.handle.net/2060/19780009781.

[11] R. Guha, M. T. Howard, G. R. Hutchison, P. Murray-Rust, H. Rzepa, C. Steinbeck, J. Wegner, and E. L. Willighagen. The blue obelisk interoperability in chemical informatics. *Journal of Chemical Information and Modeling*, 46(3):991–998, 2006. doi:10.1021/ci050400b.

[12] F. A. Hamprecht, A. J. Cohen, D. J. Tozer, and N. C. Handy. Development and assessment of new exchange-correlation functionals. *J. Chem. Phys.*, 109(15):6264–6271, October 1998. doi:10.1063/1.477267.

[13] P. J. Hay. Gaussian basis sets for molecular calculations. the representation of 3D orbitals in transition-metal atoms. *J. Chem. Phys.*, 66:4377–4384, 1977. doi:10.1063/1.433731.

[14] W. J. Hehre, R. Ditchfield, L. Radom, and J. A. Pople. Molecular orbital theory of the electronic structure of organic compounds. v. molecular theory of bond separation. *J. Am. Chem. Soc.*, 92(16):4796–4801, August 1970. doi:10.1021/ja00719a006.

[15] H. Kammler, R. Jossen, P. Morrison, S. Pratsinis, and G. Beaucage. The effect of external electric fields during flame synthesis of titania. *Powder technology*, 135(1):310–320, 2003.

[16] B. Karlemo, P. Koukkari, and J. Paloniemi. Formation of gaseous intermediates in titanium(IV) chloride plasma oxidation. *Plasma Chem. Plasma Process.*, 16:59–77, 1996. doi:10.1007/BF01465217.

[17] M. Katzer, A. Weber, and G. Kasper. The effects of electrical fields on growth of titania particles formed in a CH_4–O_2 diffusion flame. *Journal of Aerosol Science*, 32(9):1045–1067, 2001.

[18] R. Krishnan, J. S. Binkley, R. Seeger, and J. A. Pople. Self-consistent molecular-orbital methods. xx. Basis set for correlated wave-functions. *J. Chem. Phys.*, 72:650–654, 1980.

[19] J. C. Magyar, A. J. Morris, G. D. Wootten, and W. A. Yuill. Method and apparatus for producing titanium dioxide. US Patent 6,207,131, April 2006.

[20] B. J. McBride, M. J. Zehe, and S. Gordon. NASA Glenn coefficients for calculating thermodynamic properties of individual species. Technical Report TP-2002-211556, NASA, Glenn Research Center, Cleveland, OH, 2002. URL http://hdl.handle.net/2060/20020085330.

[21] A. D. McLean and G. S. Chandler. Contracted gaussian-basis sets for molecular calculations. i. 2nd row atoms, z=11-18. *J. Chem. Phys.*, 72:5639–5648, 1980.

[22] N. O'Boyle, C. Morley, and G. Hutchison. Pybel: a python wrapper for the open-babel cheminformatics toolkit. *Chemistry Central Journal*, 2(1):5, 2008. ISSN 1752-153X. doi:10.1186/1752-153X-2-5.

[23] W. Phadungsukanan, S. Shekar, R. Shirley, M. Sander, R. H. West, and M. Kraft. First-principles thermochemistry for silicon species in the decomposition of tetraethoxysilane. *J. Phys. Chem. A*, 113(31):9041–9049, Jul 2009. doi:10.1021/jp905494s.

[24] K. Raghavachari and G. W. Trucks. Highly correlated systems - excitation-energies of 1st row transition-metals Sc-Cu. *J. Chem. Phys.*, 91:1062–1065, 1989.

[25] R. Shirley, Y. Liu, T. S. Totton, R. H. West, and M. Kraft. First-principles thermochemistry for the combustion of a $ticl_4$ and $alcl_3$ mixture. *J. Phys. Chem. A*, 113(49): 13790–13796, 2009. doi:10.1021/jp905244w.

[26] G. P. Smith, D. M. Golden, M. Frenklach, N. W. Moriarty, B. Eiteneer, M. Goldenberg, C. T. Bowman, R. K. Hanson, S. Song, W. C. Gardiner, V. V. Lissianski, and Z. Qin. GRI-Mech 3.0. software package, 2008. URL http://me.berkeley.edu/gri-mech/.

[27] A. J. Wachters. Gaussian basis set for molecular wavefunctions containing third-row atoms. *J. Chem. Phys.*, 52:1033–1036, 1970. doi:10.1063/1.1673095.

[28] D. Weininger. SMILES, a chemical language and information system. 1. Introduction to methodology and encoding rules. *J. Chem. Inf. and Comput. Sci.*, 28(1): 31–36, 1988. doi:10.1021/ci00057a005.

[29] D. Weininger, A. Weininger, and J. Weininger. SMILES. 2. Algorithm for generation of unique SMILES notation. *J. Chem. Inf. Comput. Sci.*, 29(2):97–101, 1989. doi:10.1021/ci00062a008.

[30] R. H. West, G. J. O. Beran, W. H. Green, and M. Kraft. First-principles thermochemistry for the production of TiO_2 from $TiCl_4$. *J. Phys. Chem. A*, 111(18):3560–3565, 2007. doi:10.1021/jp0661950.

[31] R. H. West, M. S. Celnik, O. R. Inderwildi, M. Kraft, G. J. O. Beran, and W. H. Green. Toward a comprehensive model of the synthesis of TiO_2 particles from $TiCl_4$. *Ind. Eng. Chem. Res.*, 46(19):6147–6156, 2007. ISSN 0888-5885. doi:10.1021/ie0706414.

[32] R. H. West, R. A. Shirley, M. Kraft, C. F. Goldsmith, and W. H. Green. A detailed kinetic model for combustion synthesis of titania from $TiCl_4$. *Combust. Flame*, 156: 1764–1770, 2009. doi:10.1016/j.combustflame.2009.04.011.

[33] H. Xie, G. Gao, Z. Tian, N. Bing, and L. Wang. Synthesis of TiO_2 nanoparticles by propane/air turbulent flame CVD process. *Particuology*, 7(3):204–210, 2009. ISSN 1674-2001. doi:10.1016/j.partic.2009.03.003.